



Response of a Sandwich Plate with Auxetic Anti-tetrachiral Core to Puncture

Jakub Michalski^(✉) and Tomasz Streck

Institute of Applied Mechanics, Poznan University of Technology, Poznan, Poland
jakub.ja.michalski@doctorate.put.poznan.pl

Abstract. Auxetic materials and structures have unique properties thanks to their negative Poisson's ratio resulting from specific micro- or macrostructure. They are known to have superior resistance to dynamic loads in many cases. This includes fatigue, fracture, vibrations, blasts, and impacts. However, this topic still requires further research since there are several types of auxetics and the effect of their Poisson's ratio on the response to various dynamic loads can be unexpected. In this article, impact tests were performed using the finite element method. The behavior of two sandwich plates was compared. The first plate had an auxetic anti-tetrachiral core while the other one, used for reference, was not auxetic and had a hexagonal honeycomb core. The goal was to find out whether this type of auxetic structure can be used for improved puncture protection or not. The results obtained from numerical simulations definitely confirm that the auxetic plate has the potential to replace its hexagonal honeycomb counterpart that could be used as shielding in various demanding applications.

Keywords: Auxetics · Sandwich plates · Puncture · Explicit · Dynamics · Finite element method

1 Introduction

1.1 Auxetics and Their History

Materials with a negative Poisson's ratio are called auxetics. They deform in an unusual manner when subjected to tension (they become thicker) or compression (they become thinner). This characteristic influences the behavior of auxetics also under other operating conditions. Their improved strength and resistance to various kinds of loads result in many potential applications. It has already been proven that auxetics can be used, among others, for furniture, protection equipment, sports gear, sensors and actuators, components in the aerospace industry, implants and prostheses, gaskets, or fasteners [1, 2]. This wide range of applications continues to expand with new research in the field of auxetics. It is also important to mention that auxetic structures can be made of regular materials such as structural steel or aluminum and their negative Poisson's ratio (measured as a ratio of transverse to longitudinal strain) is a result of a specific shape. The simplest example of such a structure is a re-entrant, shaped like an hourglass and obtained directly from the regular hexagonal honeycomb cell [1]. Adjustment of its internal angle

(between the ribs of unit cells) leads to a change in the value of Poisson's ratio. Thus, the modification of this angle allows for a smooth transition to a non-auxetic structure [3]. However, there are also many other auxetic structures, including the anti-tetrachiral one used in this case.

The history of auxetics goes back to Saint-Venant's discovery that Poisson's ratio can have negative values. After that, in the XX century, scientists confirmed negative Poisson's ratio of several natural structures (including minerals and tissues) through experiments. The large interest in this type of materials began in the 1980s when tests were extended to artificial structures [1]. The development of numerical methods allowed researchers to perform their studies on those unique materials much more efficiently. One of the greatest achievements in the field of auxetics was the invention of a method of turning regular foams into auxetic ones. This approach was first described by Lakes [4] in 1987 and then improved by other scientists. The method is based on the fact that proper mechanical and thermal treatment changes the microstructure of foams and leads to a negative Poisson's ratio.

In fact, the name auxetics was not introduced until 1991 when Evans [5] derived it from the Greek word "auxetikos" meaning "the one that tends to increase". Henceforth, materials and structures with negative Poisson's ratio are commonly referred to by this name.

Nowadays, research in the field of auxetics focuses mainly on the design of new complex micro- or even nanostructures and their advanced manufacturing methods, including precise additive manufacturing methods. Apart from that, there are still several types of loads and applications where auxetics have not been thoroughly tested yet but provide promising initial results. Some of these cases, studied by authors, are fatigue [6] and blast [7] or impact conditions. The latter are discussed in this article.

1.2 Auxetic Sandwich Plates. Blast and Impact Resistance of Auxetics

Sandwich (three-layered) plates are common composite structures used in various applications requiring high strength and low weight. This makes them particularly useful in the aerospace and defense industry. Such plates consist of two outer skins and a much thicker but porous core. The core is usually made of foam but it can be also designed as a honeycomb with a selected type of unit cell. Various auxetic sandwich panels are often tested in terms of the blast, impact, crushing, or otherwise dynamic load resistance.

The increased resistance of auxetic structures to sudden localized loads such as impact or blast can be explained based on the indentation test. This kind of experiment was carried out already by Chan and Evans [8] in 1998. The authors compared conventional and auxetic foams and noticed that the latter ones behave differently. In the case of auxetic foam, the material tends to flow towards the indenter densifying around the contact area. This results in significantly higher stiffness and lower deflection under the same load. In addition, Strek et al. [9] performed numerical simulations of contact between cylinder and plate with auxetic covering layer.

Imbalzano et al. [10] performed numerical simulations on plates with a core made of unit cells in the form of a 3D beam-like re-entrant lattice. The authors confirmed that the auxetic plate undergoes significantly lower deflection than the equivalent monolithic panel. Novak et al. [11, 12] checked the response of chiral auxetic structure used as a core in the composite plate. It was proven that auxetic core may increase resistance to blast

and impact. Response of sandwich panel with chiral auxetic core to projectile impact was also verified numerically by Novak et al. [13]. Authors confirmed that the ballistic limit velocity (projectile velocity required to penetrate the structure) can be increased by introducing auxetic core.

Clearly, more previous research focuses on the blast resistance of auxetic sandwich panels and other lattice structures. Imbalzano et al. [14] compared various designs of auxetic re-entrant core with non-auxetic hexagonal honeycomb one. The authors concluded that auxetic composite panels are promising structures for applications requiring improved resistance to explosions. Al-Rifaie et al. [15] suggested that graded auxetic lattices can be used to further reinforce the blast-resistant gates. Finally, Michalski et al. [7] confirmed that sandwich plates with anti-tetrachiral core (further studied in this article) provide a significant increase in blast resistance when compared with a panel having a hexagonal honeycomb core.

Impact, crushing, and crashworthiness analyses are often performed for different types of auxetic honeycombs and other auxetic structures. Among others, Zhang et al. [16] numerically evaluated the response of re-entrant honeycomb with various cell angles subjected to dynamic crushing. Gao et al. [17] performed multi-objective crashworthiness optimization for auxetic cylindrical structure in order to increase the energy absorption.

2 Johnson-Cook Plasticity and Failure Models

2.1 Johnson-Cook Plasticity Model

Johnson-Cook plasticity model is a special form of Mises model utilizing analytical forms of hardening law and strain rate dependence. It is typically used for dynamic simulations involving the deformation of metals at high strain rates. The yield surface and flow rule in the Johnson-Cook model are the same as in the original Mises one. Isotropic hardening used in this model assumes the following relation [18–20]:

$$\sigma^0 = \left[A + B \left(\bar{\epsilon}^{pl} \right)^n \right] \left(1 - \hat{\theta}^m \right), \quad (1)$$

where: σ^0 – static yield stress, $\bar{\epsilon}^{pl}$ – equivalent plastic strain, A, B, n, m – measured material parameters, $\hat{\theta}$ – non-dimensional temperature which is:

- 0 for current temperature θ lower than transition temperature (at or below which no temperature dependence of the yield stress exists),
- $(\theta - \theta_{transition}) / (\theta_{melt} - \theta_{transition})$ for current temperature between or equal to transition temperature or melting temperature,
- 1 for current temperature higher than melting temperature.

Optionally, strain rate dependence can be included for this model. Then the yield stress at nonzero strain rate is [20]:

$$\tilde{\sigma} = \left[A + B \left(\bar{\epsilon}^{pl} \right)^n \right] \left[1 + C \ln \left(\frac{\dot{\bar{\epsilon}}^{pl}}{\dot{\epsilon}_0} \right) \right] \left(1 - \hat{\theta}^m \right), \quad (2)$$

where: $C, \dot{\epsilon}_0$ – measured material parameters, $\dot{\bar{\epsilon}}^{pl}$ – equivalent plastic strain rate.

2.2 Johnson-Cook Dynamic Failure Model

In Abaqus software, a dynamic failure model is available for use with the aforementioned Johnson-Cook plasticity. It is assumed that failure occurs when the sum of the quotients of the increment of the equivalent plastic strain and the strain at failure exceeds 1. The strain at failure is defined as [20]:

$$\bar{\varepsilon}_f^{pl} = \left[d_1 + d_2 \exp\left(d_3 \frac{p}{q}\right) \right] \left[1 + d_4 \ln\left(\frac{\dot{\varepsilon}^{pl}}{\dot{\varepsilon}_0}\right) \right] (1 + d_5 \hat{\theta}), \quad (3)$$

where: $d_1 - d_5$ – measured failure parameters, $\dot{\varepsilon}_0$ – reference strain rate, p/q – pressure-deviatoric stress ratio.

3 Research Problem

3.1 Description of the Problem and Method

For this article, finite element analyses were carried out in Abaqus 2021 software. Two designs of sandwich plates were tested – auxetic and non-auxetic one. The goal was to evaluate the response of the model with auxetic core to impact load and compare it to the results of the reference simulation with the conventional plate. Explicit dynamics analyses were performed and the impactor was assumed to be rigid.

3.2 Geometry and Mesh

Both plates were modeled in such a way to keep their overall size and unit cells dimensions as close to identical as possible. However, due to the different geometry of both types of unit cells, some discrepancy was unavoidable. The same remark also applies to the relative densities of both plates. Each panel's size was about $305 \times 305 \times 75$ mm (with two 5 mm thick skins included). The approximate size of unit cells was equal to 26 mm. Geometries of unit cells are shown in Fig. 1.

Skins were meshed with C3D8R solid elements (linear hexahedrons with reduced integration) due to their considerable thickness when compared to the thickness of cores which in turn were meshed with S4R shell elements (linear quadrilaterals with reduced integration). The mesh consisted of 22326 solid elements and 57584 shell elements (a total of 79910 elements and 82584 nodes) in the case of an auxetic plate. The conventional plate was meshed with 22326 solid elements and 58580 shell elements (a total of 80906 elements and 86954 nodes). The shell element thickness was set to 0.76 mm in both cases. All parts were positioned appropriately with respect to each other to account for shell element thickness.

In addition to panels, a rigid impactor had to be modeled. It was shaped as a hemisphere attached to a cylinder. Both the hemisphere and cylinder radius was 15 mm while the height of the cylindrical part was 30 mm. The impactor's mass was 222 g. It was meshed with 944 solid elements (C3D8R type) having a total of 1179 nodes. The impactor was placed in the middle of each plate, right above it. Meshed geometries for both analysis cases are shown in the pictures below (Fig. 2 and 3).

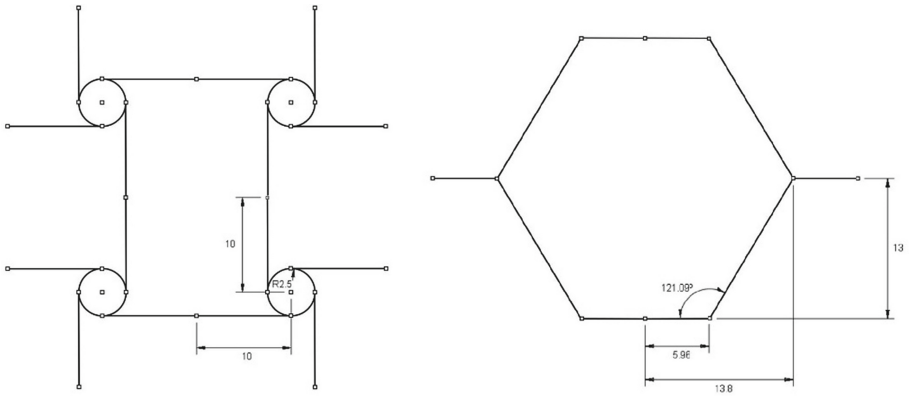


Fig. 1. Geometries of unit cells, auxetic cell on the left and non-auxetic cell on the right.

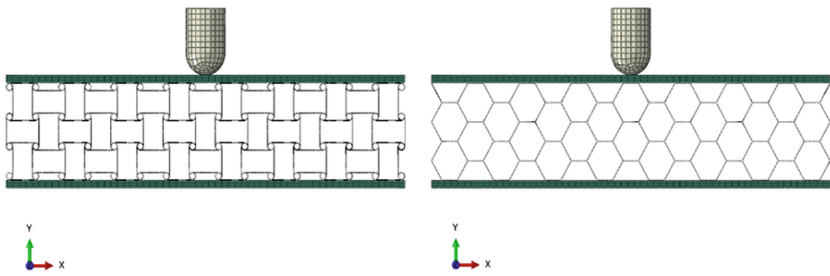


Fig. 2. Front view of meshed geometries used for both analyses, auxetic plate on the left and non-auxetic plate on the right.

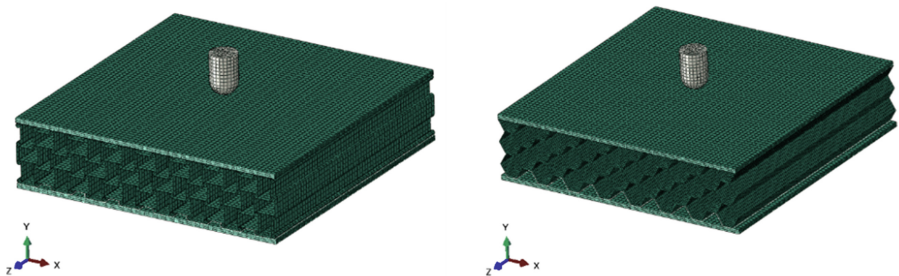


Fig. 3. Isometric view of meshed geometries used for both analyses, auxetic plate on the left and non-auxetic plate on the right.

3.3 Material Properties

It was assumed that the skins and cores of the plates are made of the same material – aluminum 6061-T6. The following material properties were defined [20, 21]:

- density: 2700 kg/m³,
- Young’s modulus: 68 GPa,
- Poisson’s ratio: 0.33,
- plasticity with Johnson-Cook hardening model: $A = 324.1$, $B = 113.8$, $n = 0.42$,
- $m = 1.34$, $\theta_{\text{melting}} = 925$ K, $\theta_{\text{transition}} = 293.2$ K,
- strain rate dependence (Johnson-Cook model): $C = 0.002$, $\epsilon_0 = 1$,
- shear failure (Johnson-Cook model): $d_1 = -0.77$, $d_2 = 1.45$, $d_3 = 0.47$, $d_4 = 0$, $d_5 = 1.6$,
- specific heat: 897 J/kg*K.

3.4 Analysis Settings

The same analysis settings were used in both cases. It was assumed that skins are attached to cores via a perfect bonding, i.e. the connection cannot fail. Thus, a tie constraint was used to attach the parts to each other. This assumption is justified by manufacturing methods that can be used for such components, e.g. extrusion. General contact functionality was used to account for the frictionless contact with impactor and self-contact within the core of each plate. Friction was ignored in this case due to the fact that its effects are expected to have small influence on the results and that accurate modeling of frictional effects requires comprehensive experimental studies. In these studies, heating effects were also omitted to reduce the already high complexity of analyses. However, those effects are planned to be verified in future works, once reliable data will be obtained through experiments.

The plates were clamped on each side. The authors could have used symmetry in this case, model only one-quarter of each plate, and apply proper boundary conditions but this approach was not necessary due to sufficient computational resources and to avoid any mistakes. However, in future studies, the use of symmetry may become necessary.

Rigid body constraint was applied to the impactor so that it was assumed to be perfectly rigid. The initial velocity of 300 m/s was applied to the impactor through its reference point placed in its center of mass. Another initial condition used in the analysis was the temperature of 273 K applied to the whole model. The analysis time was 1.5 ms.

4 Results

The results of the simulations are shown in the pictures below (Fig. 4, 5, 6, 7 and 8).

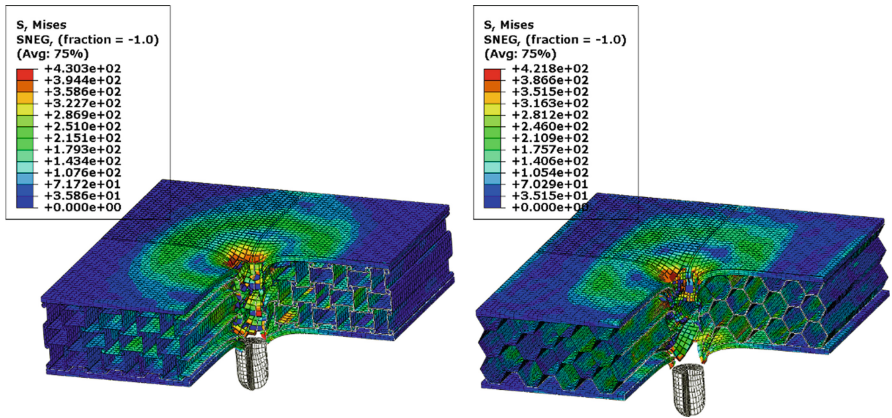


Fig. 4. Cut view of von Mises stress contour plots on the deformed shape of each model at corresponding time frames (0.625 ms), auxetic plate on the left, and non-auxetic plate on the right.

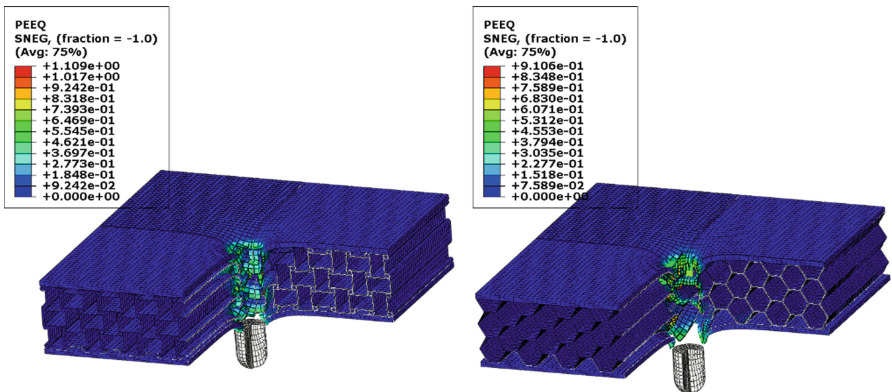


Fig. 5. Cut view of equivalent plastic strain contour plots on the deformed shape of each model at corresponding time frames (0.625 ms), auxetic plate on the left, and non-auxetic plate on the right.

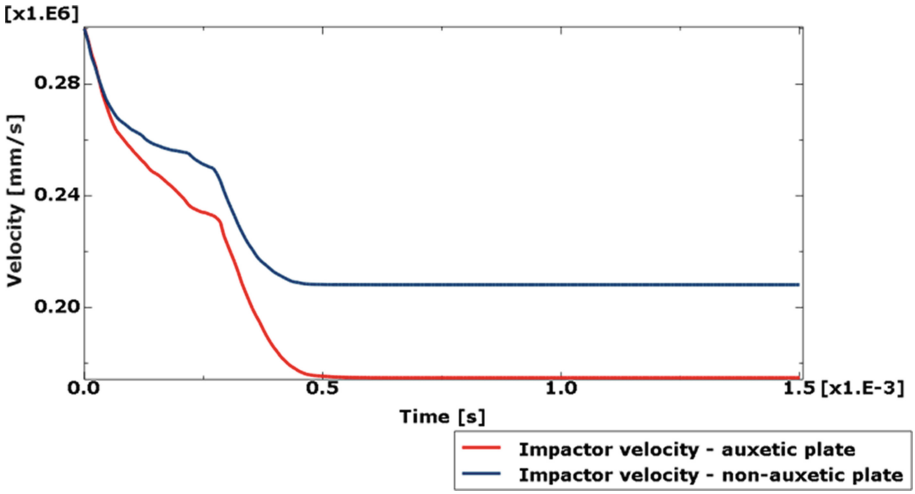


Fig. 6. Time history of impactor’s vertical velocity throughout the analysis for both cases.

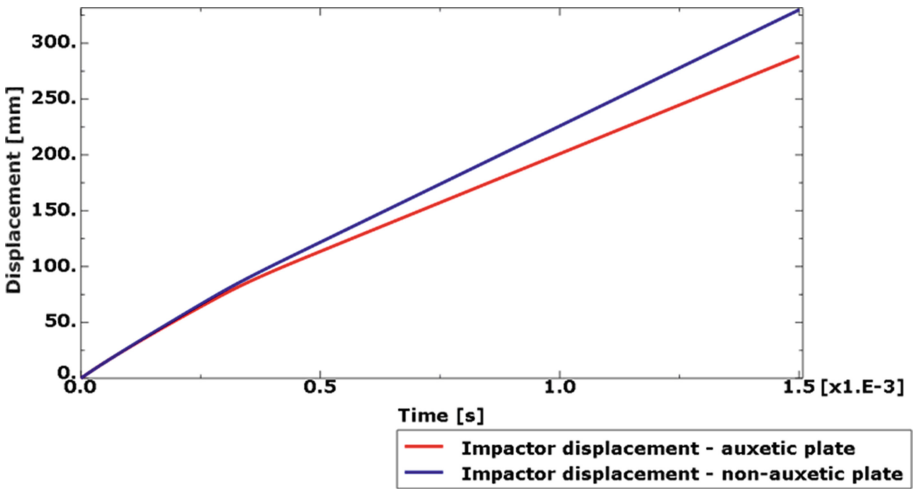


Fig. 7. Time history of impactor’s vertical displacement throughout the analysis for both cases.

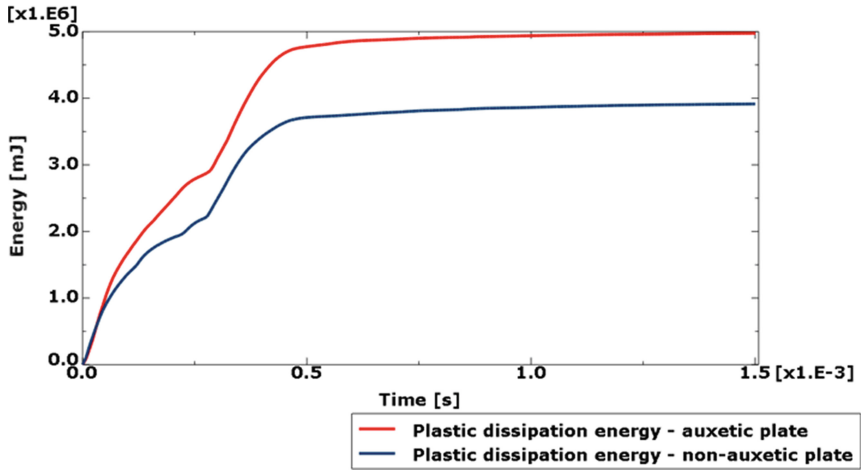


Fig. 8. Time history of plastic dissipation energy throughout the analysis for both cases.

Obtained results indicate that the auxetic anti-tetrachiral core slows down the projectile more effectively than the non-auxetic core. Stresses and plastic strains in both cases are similar but the key factor for evaluation of the performance of both plates subjected to impact is the residual velocity of the impactor. Total plastic dissipation energy was also compared for both cases to verify the energy absorption capabilities of the plates. It was found that the auxetic core increases plastic dissipation.

In order to confirm that these relationships hold regardless of the unavoidable difference in masses mentioned before, authors performed additional studies. Thickness of shell elements forming cores was adjusted in such a way that both plates had the same mass (around 1725 g). The results of this study are presented below (Fig. 9, 10 and 11).

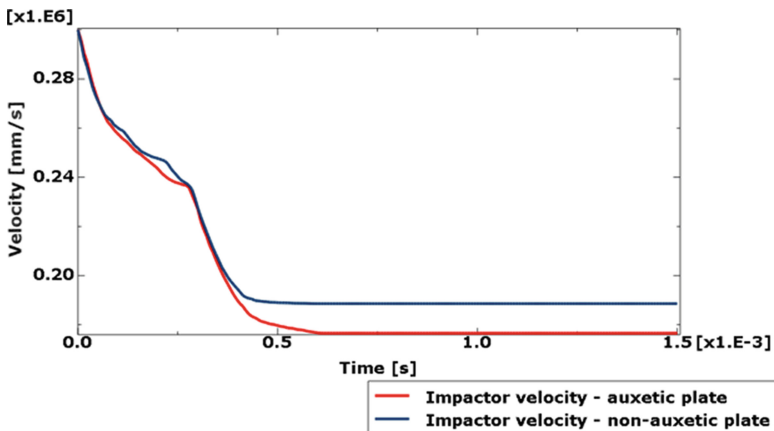


Fig. 9. Time history of impactor's vertical velocity throughout the analysis for both cases with equalized masses.

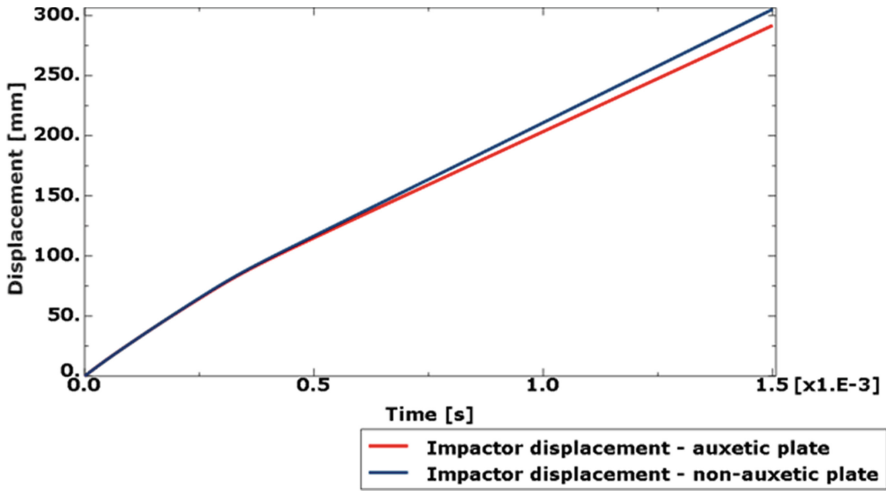


Fig. 10. Time history of impactor’s vertical displacement throughout the analysis for both cases with equalized masses.

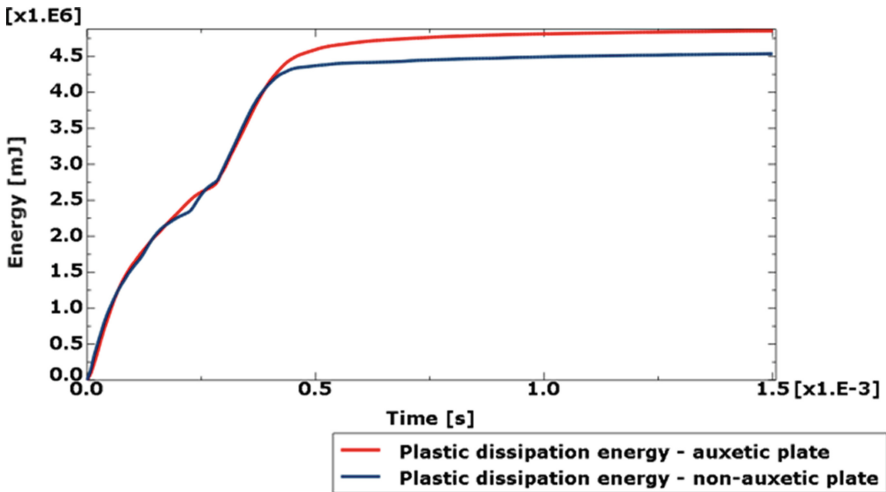


Fig. 11. Time history of plastic dissipation energy throughout the analysis for both cases with equalized masses.

It can be seen that the relationships are not invalidated with equalization of masses of the plates.

The authors also performed the analyses with plates having the same overall size as in previous studies but with doubled number of layers of unit cells. The cells were thus smaller and additional effects could be checked. The results of those analyses are presented below (Fig. 12, 13 and 14).

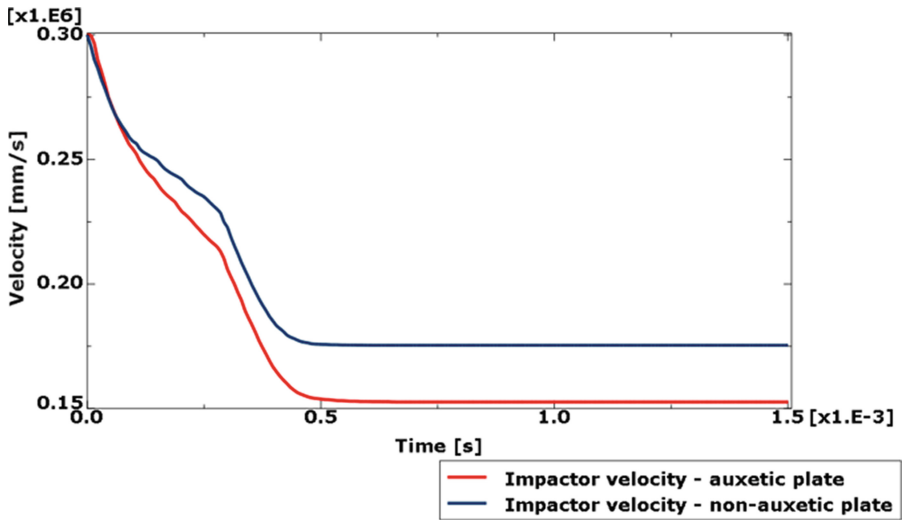


Fig. 12. Time history of impactor's vertical velocity throughout the analysis for both cases with more unit cells.

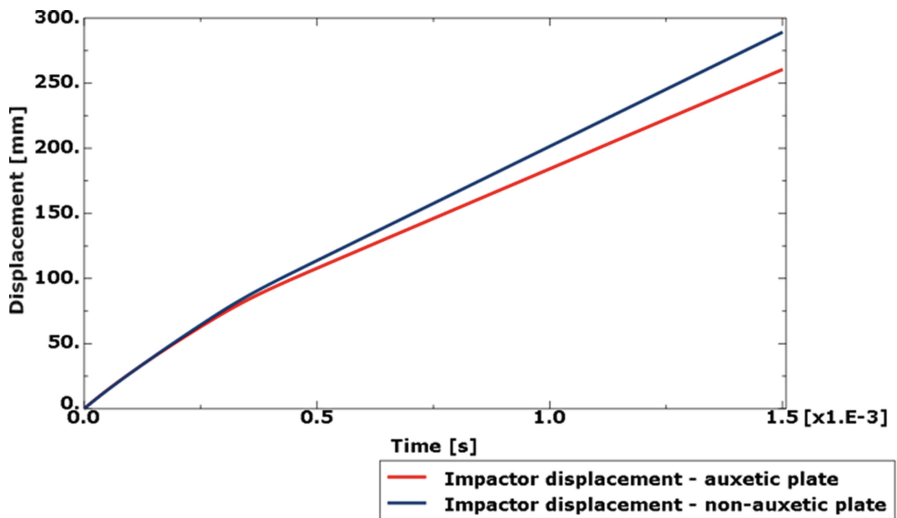


Fig. 13. Time history of impactor's vertical displacement throughout the analysis for both cases with more unit cells.

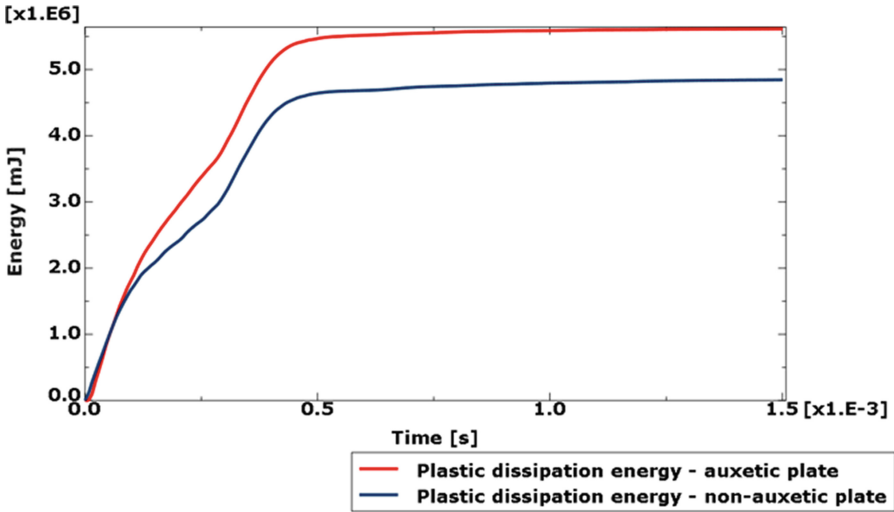


Fig. 14. Time history of plastic dissipation energy throughout the analysis for both cases with more unit cells.

The same relationships between the results can be observed also in the case of larger number of unit cells.

5 Discussion and Conclusions

Results obtained from the simulations prove that the auxetic anti-tetrachiral core performs better in terms of response to puncture than the non-auxetic hexagonal honeycomb core.

However, it is important to mention that various simplifications were used in the numerical model. There are several sources of potential errors. Mesh density was carefully selected to avoid significant dependency of the results on the level of discretization. In this case, the material model was crucial for accurate output. Because of that, material data had to be taken from reliable source. Another approximation used in the simulations is the connection between skins and cores of both plates. It was assumed that this connection cannot break during the analysis. To model it more realistically, it would be necessary to account for the potential delamination and failure of the connection. But such an approach would require additional data regarding the strength of the adhesive.

Comparison of the numerical results to data acquired from physical tests could provide interesting insights into the problem being considered here. However, in cases of impact loading, experiments are difficult to perform and potentially dangerous. This is especially true for significant projectile velocities, as is the case here. Thus, numerical methods are often used when evaluating the impact resistance of various structures.

Results obtained for the purpose of this article confirm that, in analyzed conditions, auxetic anti-tetrachiral core can be used in place of the regular hexagonal honeycomb structure to increase the puncture protection capabilities of sandwich plates. Such panels

could be used in various protective structures, among others for the aerospace and defense industry where lightweight honeycomb structures are already used but may still require further strengthening against high-velocity impacts.

Acknowledgments. This work was supported by grant of the Ministry of Science and Higher Education in Poland: 0612/SBAD/3576 (2021/2). Simulations were carried out during an internship in BudSoft company.

References

1. Lim, T.C.: *Auxetic Materials and Structures*. Springer, Singapore (2015)
2. Ren, X., Das, R., Tran, P., Ngo, T.D., Xie, Y.M., Auxetic metamaterials and structures: a review. *Smart Mater. Struct.* **27**(2), 023001 (2018)
3. Bilski, M., Piękowski, P.M., Wojciechowski, K.W.: Extreme Poisson's ratios of honeycomb, re-entrant, and zig-zag crystals of binary hard discs. *Symmetry* **13**(7), 1127 (2021)
4. Lakes, R.: Foam structures with negative Poisson's ratio. *Science* **235**(4792), 1038–1040 (1987)
5. Evans, K.E.: Auxetic polymers: a new range of materials. *Endeavour* **15**(4), 170–174 (1991)
6. Michalski, J., Streck, T.: Fatigue life of auxetic re-entrant honeycomb structure. In: Gapiński, B., Szostak, M., Ivanov, V. (eds.) *MANUFACTURING 2019. LNME*, pp. 50–60. Springer, Cham (2019). https://doi.org/10.1007/978-3-030-16943-5_5
7. Michalski, J., Streck, T.: Blast resistance of sandwich plate with auxetic anti-tetrachiral core. *Vib. Phys. Syst.* **31**(3), 20317 (2020)
8. Chan, N., Evans, K.E.: Indentation resilience of conventional and auxetic foams. *J. Cell. Plast.* **34**(3), 231–260 (1998)
9. Streck, T., Matuszewska, A., Jopek, H.: Finite element analysis of the influence of the covering auxetic layer of plate on the contact pressure. *Phys. Status Solidi B* **254**(12), 1700103 (2017)
10. Imbalzano, G., Tran, P., Ngo, T.D., Lee, P.V.S.: Three-dimensional modelling of auxetic sandwich panels for localized impact resistance. *J. Sandwich Struct. Mater.* **19**(3), 291–316 (2017)
11. Novak, N., Starcevic, L., Vesenjaj, M., Ren, Z.: Blast and ballistic loading study of auxetic composite sandwich panels with LS-DYNA. In: *12th European LS-DYNA Conference 2019, Koblenz, Germany* (2019)
12. Novak, N., Starcevic, L., Vesenjaj, M., Ren, Z.: Blast response study of the sandwich composite panels with 3D chiral auxetic core. *Compos. Struct.* **210**, 167–178 (2019)
13. Novak, N., Vesenjaj, M., Kennedy, G., Thadhani, N., Ren, Z.: Response of chiral auxetic composite sandwich panel to fragment simulating projectile impact. *Phys. Status Solidi B* **257**(10), 1900099 (2020)
14. Imbalzano, G., Linforth, S., Ngo, T.D., Lee, P.V.S., Tran, P.: Blast resistance of auxetic and honeycomb sandwich panels: comparisons and parametric designs. *Compos. Struct.* **183**, 242–261 (2018)
15. Al-Rifaie, H., Sumelka, W.: Improving the blast resistance of large steel gates—numerical study. *Materials* **13**(9), 2121 (2020)
16. Zhang, X., Ding, H., An, L., Wang, X.: Numerical investigation on dynamic crushing behavior of auxetic honeycombs with various cell-wall angles. *Adv. Mech. Eng.* (2015)
17. Gao, Q., Zhao, X., Wang, C., Wang, L., Ma, Z.: Multi-objective crashworthiness optimization for an auxetic cylindrical structure under axial impact loading. *Mater. Des.* **143**, 120–130 (2018)

18. Stopel, M.: Methodology for determining constants for Johnson-Cook constitutive and damage model. University of Sciences and Technology in Bydgoszcz, Bydgoszcz (2020). (in Polish)
19. Jankowiak, T.: The use of experimental methods and computer simulation for determining the properties of materials subjected to high deformation rate. Poznan University of Technology, Poznan (2016). (in Polish)
20. Dassault Systemes SIMULIA Abaqus: 2021 software documentation
21. Dassault Systemes SIMULIA Abaqus Technology Brief: Simulation of the ballistic perforation of aluminum plates with Abaqus/Explicit